Regular Article

PHYSICAL CHEMISTRY RESEARCH
Published by the
Iranian Chemical Society
www.physchemres.org
info@physchemres.org

Phys. Chem. Res., Vol. 8, No. 4, 755-765, December 2020
DOI: 10.22036/pcr.2020.217674.1724

Ejection Time of a Semi-Flexible Polymer from Strong Confinement inside a Nano-slit

F. Hafizi, S.M. Hoseinpoor and N. Nikoofard*

Institute of Nanoscience and Nanotechnology, University of Kashan, Kashan 51167-87317, Iran

(Received 28 January 2020, Accepted 9 August 2020)

Advances in nano-fabrication techniques have enabled confinement of polymers at nano-scale cavities. This has raised a higher demand for development of theories for polymers in severe confinements. In this manuscript, the escape of a polymer confined in a nano-slit through a nano-pore in the strong confinement regime is investigated theoretically and by using Langevin Dynamics (LD) simulations. The strong confinement occurs when the height of the nano-slit becomes smaller than the persistence length of the polymer. Persistence length is a measure of the polymer stiffness. The radius of gyrations R_g, the confinement force on the polymer f, and the ejection time of the polymer τ are obtained in different values of the polymer length L, the height of the nano-slit D, and the persistence length of the polymer P; the simulation results are well described with the scaling relations $\frac{R_g}{L^{0.75}} \sim (\frac{P}{D})^{0.25}$, $\frac{f}{L} \sim (\mathrm{PD}^5)^{-0.4}$ and $\frac{\tau}{L^2} \sim (\mathrm{PD}^2)^{0.42}$, respectively. The simulation results are in a rather good agreement with the theory. It seems that the relative difference between theory and simulation is due to being close to the transition region between weak and strong confinement regimes.

Keywords: Semi-flexible polymer, Nano-slit confinement, Strong confinement, Odijk regime

INTTRODUCTION

In the past decades, advances in nano-technology have enabled confinement of polymers in various nano-scale geometries [1,2]. The applications vary from examining theories for describing the polymer behavior and obtaining new insights into biological phenomena to fast DNA and protein sequencing [3,4]. There are three common types of confinement: slit-like, cylindrical, and spherical; which reduce the available dimensions for the polymer to two, one, and zero dimension(s), respectively. Other types of confinement, *e.g.* cone-shaped channels, are also studied [5]. The free energy and extension of flexible polymers in confinement is known previously from polymer science [6]. Previously-known theories [7,8] and new aspects such as spherical confinement [9] and knotting behavior [10,11] are examined using simulations and experiments.

*Corresponding author. E-mail: nikoofard@kashanu.ac.ir

The important macro-molecule, double-stranded DNA with the large persistence length of 50 nm is severely confined, *e.g.* in the cell nucleus and inside the viral capsid. As a result, confinement of polymers in length scales smaller than their persistence length is considered in the literature [12,13]. The problem of a semi-flexible polymer in confinement is more complicated because of the existence of a new length scale (persistence length) in the system, which should be compared with the size of the confining geometry. Strong confinement occurs when the size of the confining geometry becomes smaller than the polymer persistence length. New theories are developed to describe behavior of semi-flexible polymers in strong confinement [14,15,16]. Besides, organization of semi-flexible polymers [17,18] and some dynamical features such as their knotting [19] or looping [20] behavior in confinement have been the subject of research.

Theories for semi-flexible polymers are well developed and examined for slit-like and cylindrical confinements

[12,13,21,22]. The well-known de Gennes regimes (or moderate confinement) is true as long as the size of the confining geometry is much larger than the persistence length of the polymer. When the persistence length becomes smaller than the size of the confining geometry, transition to the Odijk regime (or strong confinement) is observed. Other intermediate regimes, such as the extended de Gennes regime are observed between the de Gennes and Odijk regimes in slit-like and cylindrical confinements [23].

Polymer release out of confined geometries is significant in phenomena such as drug delivery, gene therapy and understanding viral genome ejection [24]. Polymer escape from confined geometries is one kind of forced polymer translocation. Many experimental, simulation and theoretical studies have been performed on the problem of polymer translocation through a nano-pore in the past two decades [25-29]. Polymer translocation is important in bio-polymer separation [30] and analysis [31], and understanding biological phenomena [32]. Different time scales are described in the polymer translocation, involving capture and passage times [33,34]. Among different time scales, the passage time is the most studied one, which is the required time for the polymer to completely pass through the nano-pore. Besides, two types of polymer translocation are considered, un-forced [35] and forced [36] translocations. The scaling relations for the passage time in the two types of polymer translocation are obtained theoretically and by using simulations [36,37].

Polymer translocation out of a confining geometry is driven by the gain in conformational entropy of the polymer [38,39]. Different factors such as the size of the confining geometry and the persistence length of the polymer affect the ejection process. There are also other determining factors in practical situations, such as the presence of knots [40], chaperons [41] or the organization of the polymer [42]. Polymer translocation into confinement is also considered [43,44], which is related to viral genome packaging [45]. Despite extensive studies in this field, translocation of semi-flexible polymers out of confining geometries is less investigated.

In this manuscript, translocation of a single polymer out of planar confinement is studied in the Odijk regime. The polymer is initially confined in a slit geometry with a size smaller than two times of the persistence length of the polymer. The radius of gyration and the confinement force on the polymer is obtained theoretically and compared with the results of the LD simulations. Then, the polymer is allowed to escape from the confinement through a narrow pore. The passage time required for the polymer to completely escape from the confinement is obtained theoretically and by using LD simulations. Comparison between the theory and simulation results shows a relative agreement.

The theory of a polymer in slit-like confinement is reviewed in the next section that is followed by the Simulation Method and Simulation Results. The results are summarized in the last section.

Theory

The radius of gyration of an un-confined polymer is obtained by $R_g \sim V^{\frac{1}{5}} b^{\frac{2}{5}} N^{\frac{3}{5}}$, according to the Flory theory. For a polymer with non-zero persistence length, the effective monomers are described by a cylinder of length b = 2P and width σ . N is the number of monomers, which is related to the contour length of the polymer, L = Nb. The excluded volume of a cylindrical monomer is obtained from the virial expansion $V = b^2\sigma$. Thus, the radius of gyration of the free polymer becomes $R_g \sim L^{\frac{3}{5}} P^{\frac{1}{5}} \sigma^{\frac{1}{5}}$ [6].

In the problem of a confined polymer, there are three length scales in the system: the radius of gyration R_g, the persistence length P and the size of the confining geometry D. For a polymer confined in a nano-slit, D is the distance between the two plates or the height of the nano-slit (Fig. 1). In weak confinement $D \approx 3R_g$, the polymer feels the confining geometry very weakly. In moderate confinement $2P << D < R_g$ (the de Gennes regime), the blob theory is used in which the polymer is described as a sequence of blobs (Fig. 1a). When $D << 2P$, the polymer is in the strong confinement or the Odijk regime (Fig. 1b). In this regime, the polymer is divided into a sequence of deflection segments.

In the de Gennes regime, the polymer is divided into blobs of size D. Inside the blobs, the monomers have an un-perturbed statistics $D \sim L_b^{\frac{3}{5}} P^{\frac{1}{5}} \sigma^{\frac{1}{5}}$, where L_b is the contour length of the polymer inside the blobs. Free energy of the polymer ΔF is equal to the Boltzmann energy k_BT

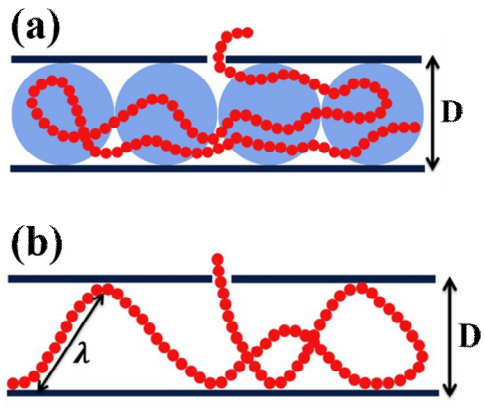

Fig. 1. Schematics of a polymer in slit confinement. (a) Confinement in the de Gennes regime, $2P << D < R_g$, is described by the blob theory. The size of the blobs (large spheres) is equal to the size of the nano-slit. (b) Confinement in the Odijk regime, $\sigma < D < 2P$, is described by the deflection theory. The contour length of the polymer between two deflections is shown with λ.

times the number of blobs, $\frac{L}{L_B}$; $\Delta F \sim k_B T \frac{L}{L_B} \sim k_B T L D^{-\frac{5}{3}} P^{\frac{1}{3}} \sigma^{\frac{1}{3}}$. Taking the derivative of the free energy with respect to D gives the confinement force on the polymer from the walls of the nano-slit; $f \sim k_B T L D^{-\frac{8}{3}} P^{\frac{1}{3}} \sigma^{\frac{1}{3}}$. The radius of gyration of the polymer in the plane of the slit is found from a self-avoiding walk of the blobs in 2D; $R_g \sim D\ (\frac{L}{L_b})^{\frac{3}{4}}$. This gives $R_g \sim L^{\frac{3}{4}} D^{-\frac{1}{4}} P^{\frac{1}{4}} \sigma^{\frac{1}{4}}$ [6].

To be precise, the Odijk regime is defined when $\sigma < D < 2P$ in this manuscript. In the Odijk regime, the polymer contour is deflected when it approaches the walls of the nano-slit (Fig. 2b). The size of the contour length of the polymer between deflection points is given by $\lambda \sim D^{\frac{2}{3}} P^{\frac{1}{3}}$ [46]. Free energy of the confined polymer is equal to the Boltzmann energy $k_B T$ times the number of deflection segments, $\Delta F \sim k_B T \frac{L}{\lambda} \sim k_B T \frac{L}{D^{\frac{2}{3}} P^{\frac{1}{3}}}$ [21]. The confinement force on the polymer is found from the derivative of the free energy with respect to the size of the confinement;

$$f \sim k_B T \frac{L}{D^{\frac{5}{3}} P^{\frac{1}{3}}} \quad (1)$$

The radius of gyration of the polymer is obtained from a Flory type theory, considering the entropic and interaction terms of the free energy $\frac{F}{k_B T} \sim \frac{R_\parallel^2}{LP} + \frac{\lambda^2 (\frac{L}{\lambda})^2}{R_\parallel^2 D}$. Minimizing the free energy with respect to $R_\parallel$ gives

$$R_g \sim L^{\frac{3}{4}} D^{-\frac{1}{4}} P^{\frac{1}{4}} \sigma^{\frac{1}{4}} \quad (2)$$

The above relation is similar to the relation obtained for the radius of gyration in the de Gennes regime [23].

It is shown previously that the ejection time is proportional to the inverse of the confinement free energy [38]. Also, the passage time in forced polymer translocation is proportional to the inverse of the driving force [36]. For a polymer confined in a nano-slit, the driving force for the ejection process can be found from the derivative of the free energy with respect to the contour length. As a result, the ejection time for the Odijk regime becomes

$$\tau \propto D^{2/3} P^{1/3} \quad (3)$$

Simulation Method

The behavior of a semi-flexible polymer confined in a nano-slit is investigated using LD simulations. The polymer is modeled by spherical monomers which have excluded

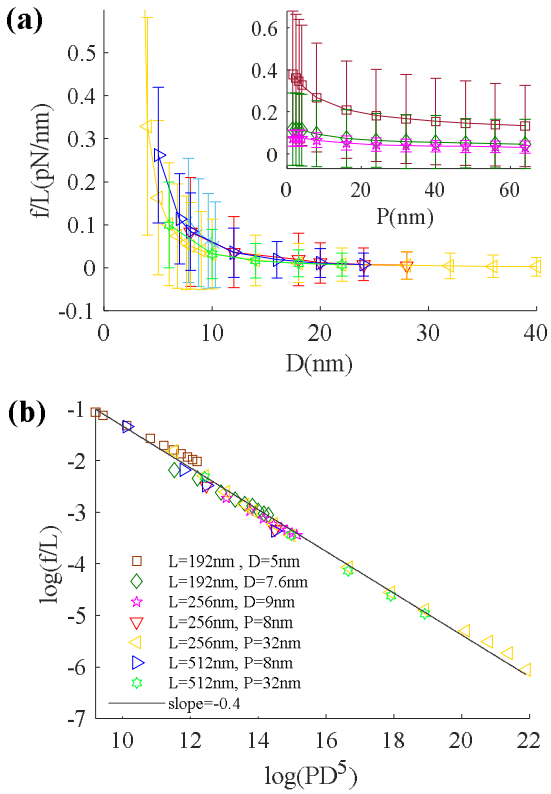

Fig. 2. (a) Confinement force *versus* the height of the nano-slit. Inset: Confinement force *versus* persistence length. (b) Log-log plot of the previous plots with re-scaled coordinates. Only data points that are in the Odijk regime are shown.

volume interactions with each other and with the walls of the nano-slit, through the shifted Lennard-Jones potential $V_{LJ}(r) = 4\varepsilon\left((\frac{\sigma}{r})^{12} - (\frac{\sigma}{r})^{6} + \frac{1}{4}\right)$. The potential is truncated at $r_{cut} = 2^{\frac{1}{6}}\sigma$. Here, ε and σ are the energy and the length scales of the simulations. The monomers are connected to each other *via* the FENE potential $V(r) = -\frac{1}{2}K\Delta r_{\max}^2 \ln\left[1 - (\frac{1}{\Delta r_{\max}})^2\right]$, where $K = 70\frac{\varepsilon}{\sigma}$ and Δ_{rmax} = 1.5σ are the bond stiffness and the maximum bond extension, respectively. The bond angle potential $V(\alpha) = K_\alpha[1 - \cos(\alpha - \pi)$ is applied, in which the stiffness determines the persistence length, $\frac{K_\alpha}{k_B T} = \frac{P}{\sigma}$.

The monomers interact with the walls of the nano-slit, through the same shifted truncated Lennard-Jones potential, in which r is the perpendicular distance between the monomers and the wall. As a result, the wall thickness is equal to σ. The length of the pore is equal to the wall thickness. The internal diameter of the pore is taken equal to 2.6σ, in accordance with Ref. [38]. For this diameter of the pore, one monomer can be inside the pore, at each time. So, the monomers should exit the nano-slit consecutively. Increasing the nano-pore diameter beyond this limit can have a dramatic effect on the results.

The Langevin equation $m\frac{dv(t)}{dt} = F(t) - \gamma m v(t) + \xi(t)$ is integrated to find the time evolution of the system. In this equation, m and v(t) are the mass and velocity of the monomers, respectively. F(t) is the force from the interaction with other monomers and the nano-structure. γmv(t) and ξ(t) are the friction and random forces, respectively. The random force is a Gaussian white noise

with a mean value that depends on the temperature. The equation of motion is integrated using the velocity-Verlet algorithm in ESPResSo 3.2.0 [47], with a time step equal to $0.01\tau_0$, where $\tau_0 = \sqrt{\frac{m\sigma^2}{\varepsilon}}$ indicates the simulation time unit. The values $\gamma = \frac{1.0}{\tau_0}$ and $T = 1.0\frac{\varepsilon}{k_B}$ are used for the damping constant and the system temperature in the Langevin equation.

Parameter values are chosen according to double-stranded DNA. σ = 2 nm (the width of DNA helix) and ε = k_BT are used, which gives the force unit of the simulation equal to 2.07pN. Each nucleotide has a length 0.34 nm; so, each bead contains $2 \times \frac{2.0\ nm}{0.34\ nm}$ nucleotides. Using the averaged molar mass of one nucleotide, 487 g mol^{-1}, the mass of each bead is found to be 9.6×10^{-26} kg. This gives the time unit of the simulations, 0.96 ns.

At the beginning of the simulations, monomers of the polymer are located between the walls according to a pruned self-avoiding random walk. Then, the polymer is equilibrated in a time of order N^2. After equilibration, the averages for the radius of gyration of the polymer and the confinement force on the polymer are calculated in a time equal to $4N^2$. The radius of gyration is found using the relation $R_{\parallel}^2 = \frac{1}{N}\sum_{i=1}^{N}[(x_i - x_{cm})^2 + (y_i - y_{cm})^2]$, where $x_i(y_i)$ and $x_{cm}(y_{cm})$ are the coordinates of the monomers and the center of mass of the polymer, respectively. The confinement force on the polymer is obtained using the overall force on the walls of the nano-slit.

For the ejections process, N - 2 monomers of the polymer are placed randomly inside the nano-slit. One monomer is placed inside the nano-pore and the other one is taken outside the nano-pore. Increasing the length of the nano-pore decreases the number of monomers inside the nano-slit and slightly affects the osmotic pressure inside the nano-slit, which is the driving force for the ejection process. The monomer inside the nano-pore is fixed during the equilibration. After equilibration, the monomer is unfixed and the simulation time is set to zero. The ejection time is recorded when all of the monomers have passed the nano-pore. For each set of parameters, 100 realizations are performed and the mean ejection time is reported. Simulations in which the first monomer returns to the space between the walls and loses the nano-pore are not taken into account (failed simulations).

The results of the simulations are compared with the theory, by fitting the theoretical equations to the simulation data. The quality of the fit is described by the root mean square error and the R squared. If one shows the data points with y_i and the estimated values from the fit with $\hat{y}_i$, the root mean square error is defined by $RMSE = \sqrt{\frac{1}{n}\sum_{i=1}^{N}(y_i - \hat{y}_i)^2}$ and the R squared by $R^2 = 1 - \frac{SSE}{TSS}$. Here, $SSE = \sum_{i=1}^{N}(y_i - \hat{y}_i)^2$ is sum of the squared errors and $TSS = \sum_{i=1}^{N}(y_i - \bar{y}_i)^2$ is the total sum of the squares, where $\bar{y}_i = \frac{1}{n}\sum_{i=1}^{n} y_i$. R squared is between 0 and 1 and is a measure of the percentage of data points explained with the fit.

SIMULATION RESULTS

Confinement Force

The error-bar plots of the confinement force on the polymer versus the height of the nano-slit and the polymer persistence length are shown in Fig. 2a and its inset, respectively. It is observed that the error-bars are large. Indeed, the values of the confinement force show large variations at each time unit of the simulations, such that most of the recorded values are zero. It is observed that the size of the error-bars can be reduced by using window-averaging (not shown on the plots). The size of the error-bars depends dramatically on the size of the window. Longer runs with large window sizes can reduce the error-bars.

For data points in the Odijk regime, the log-log plot with re-scaled coordinates is shown in Fig. 2b. It is seen all data points for various polymer lengths, persistence lengths and heights of the nano-slit converge on a master curve, by re-scaling the coordinates according to Eq. (1). A linear fit gives a slope of 0.4, which is nearly close to the theoretical value 1/3 predicted by Eq. (1). The quality of the fit is described by RMSE = 0.93 and R^2 = 0.99. RMSE is sufficiently small as the plot shows. R^2 is also close to 1,

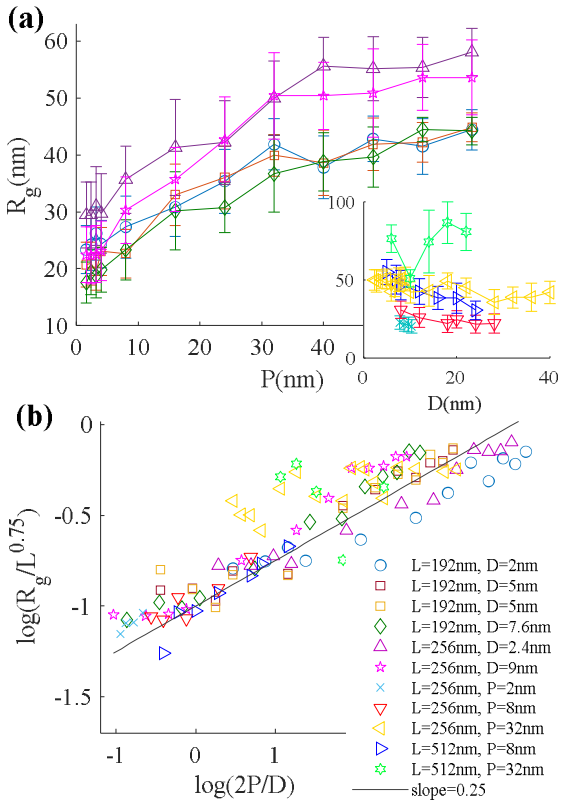

Fig. 3. (a) Radius of gyration versus height of the nano-slit. Inset: Radius of gyration versus persistence length. (b) Log-log plot of the previous plots with re-scaled coordinates.

indicating that most of the data points are described with the fit.

Chain Size

The error-bar plots of the radius of gyration *versus* the persistence length and the height of the nano-slit are shown in Fig. 3a and its inset, respectively. The error-bars are again large, specifically compared to previous studies [23]. This shows the requirement for longer simulations, which is hardly accessible with our machines (with Intel Core i7-5820K Processors). The log-log plot of data points with re-scaled coordinates is shown in Fig. 3b. It is observed that by re-scaling the coordinates according to Eq. (2), all data points with various polymer lengths, persistence lengths and heights of the nano-slit fall on a single master curve. A line with slope 0.25 can follow the data points very well, in agreement with Eq. (2). It should be declared that the radius of gyration is described with the same relation in the Odijk and de Gennes regimes [23]. In Fig. 3(b), data points with $\log(\frac{2P}{D})$ smaller than zero are in the de Gennes regime.

Ejection Time

The error-bar plots of the ejection time versus the persistence length and the height of the nano-slit are shown in Fig. 4a and its inset. The large error-bars are due to the small number of ejection times obtained from the simulation. The number of failed simulation increases with the height of the nano-slit and the persistence length. This requires a higher number of simulations, which is not accessible due to computational limitations. The log-log plot of the previous plots with re-scaled coordinates are shown in Fig. 4b. The x-coordinate is re-scaled according to the right hand side of Eq. (3). For re-scaling the

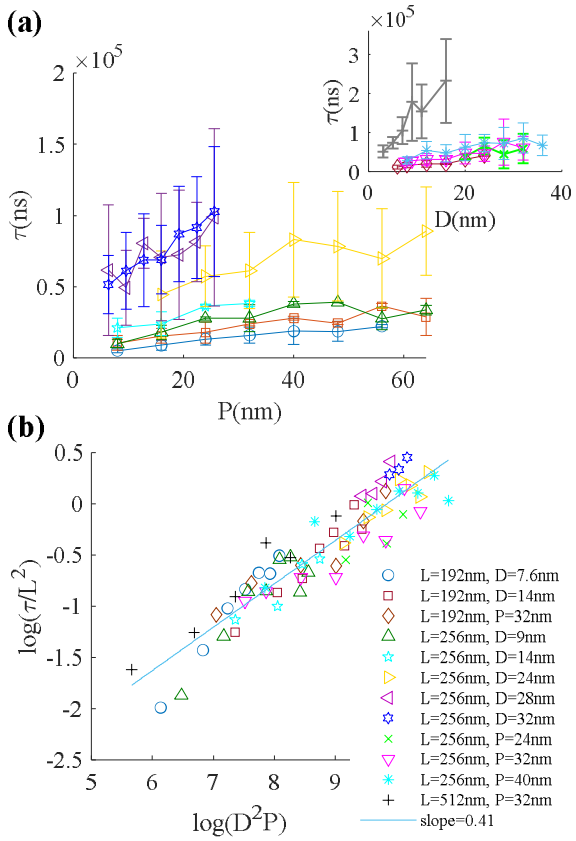

Fig. 4. (a) Ejection time of polymer from the nano-slit *versus* the height of the nano-slit. Inset: Ejection time of polymer from the nano-slit *versus* persistence length of the polymer. (b) Log-log plot of the previous plots with re-scaled coordinates. Only data points that are in the Odijk regime are shown.

y-coordinate, dividing the ejection time to N^2 gives a better convergence compared to $N^{1.6}$. Thus, according to Ref. [36], a polymer confined in a nano-slit in the Odijk regime behaves similar to a rod-like polymer rather than an excluded volume chain. The converged data points are well described with a line of slope 0.42, this is in a relative agreement with the power 1/3 predicted by Eq. (3). The quality of the fit is described with RMSE = 1.72 and $R^2 = 0.86$ which are relatively good.

Discussion on the Transition Region

To be precise, a confined polymer in a nano-slit (or nano-channel) experiences several regimes as the size of confinement decreases: de Gennes, extended de Gennes, Odijk and non-self-crossing Odijk regimes. The extended de Gennes regime occurs when $2P < D < \frac{P^2}{\sigma}$. The cross-over from the extended de Gennes to the Odijk regimes happens when D < 2P. The non-self-crossing Odijk regime occurs when D < 2σ [23]. Thus, it is not related to the present study. The relative difference between the simulation results and the theory might be due to the fact that the data points are close to the cross-over between the extended de Gennes and the Odijk regimes. It is also possible to define a transition region between these two regimes.

The polymer free energy in the transition region (from extreme D << P to moderate D >> P confinement) has been obtained previously [21];

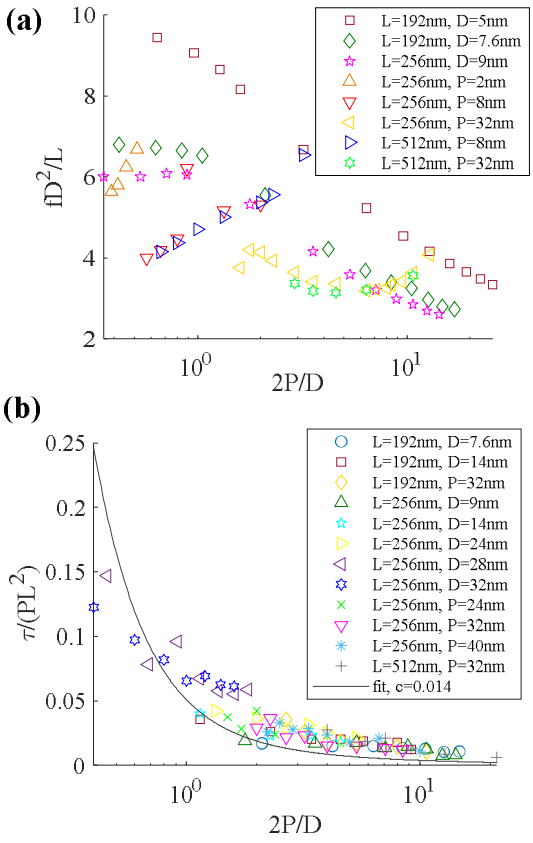

Fig. 5. (a) The re-scaled confinement force *versus* the ratio of the Kuhn length to the size of the nano-slit. (b) The re-scaled ejection time *versus* the ratio of the Kuhn length to the size of the nano-slit. Data points with 2P/D smaller than 1 are in the de Gennes regime.

$$\frac{\Delta F}{k_B T} = \frac{\pi^2 L}{6}\frac{L}{P}\frac{(\frac{P}{D})^2}{\left[1.29(\frac{P}{D})^2 + 0.99(\frac{P}{D}) + 1\right]^{\frac{2}{3}}} = \frac{L}{P}\Psi(\frac{P}{D}) \qquad (4)$$

Here, Ψ is a function of $\frac{P}{D}$. Taking the derivative of Eq. (4) with respect to D gives the confinement force as $f\frac{D^2}{L} = \Xi(\frac{P}{D})$, where Ξ is again a function of $\frac{P}{D}$. Using Eq. (4) and introducing a proportionality constant, the ejection time is found to be

$$\tau \sim c\frac{L^2}{\frac{\partial \Delta F}{\partial L}} \sim cL^2 P\psi^{-1}(\frac{P}{D}) \qquad (5)$$

The re-scaled plots for the confinement force are shown in Fig. 5a, which are not converged on a single curve. However, with re-scaling the coordinates for the ejection time, according to Eq. (5), all the data points converge on a master curve (Fig. 5b). This convergence is observed for all data points, which are in both the Odijk and the extended de Gennes regimes. Fitting with only one parameter (the proportionality constant in Eq. (5) can follow the data relatively well. The relative difference may be due to finite chain effects, because Eq. (5) is obtained in the limit of long chains.

CONCLUSIONS

The radius of gyration and the confinement force on a polymer confined in a nano-slit were obtained theoretically and by using LD simulations. The confinement force was

theoretically obtained from the derivative of the confinement free energy with respect to the height of the nano-slit. The results of LD simulations for the radius of gyration of the polymer were in a good agreement with the theory. A relative agreement between theory and simulation results was observed for the confinement force on the polymer.

The polymer was allowed to escape from the slit confinement through a nano-pore and the ejection time was measured in LD simulations. Theoretically, the ejection time was taken proportional to the inverse of the confinement free energy. The results of the simulations and the theory for the ejection time were in a relatively good agreement. Our simulation results showed that the ejection process of a polymer in the Odijk regime is similar to the forced translocation of rod-like polymers [36].

An improvement in the confinement free energy was also discussed, because the data points from LD simulations are taken from the transition region between the Odijk and de Gennes regimes. This improvement could describe the ejection time; however, the simulation results for the re-scaled confinement force did not converge on a master curve. The controversy between the confinement force and the theory may be due to the fact that the theories are obtained for infinitely long polymers. Despite this limitation, it is interesting that the theory is able to describe the ejection time well.

The present work discussed the ejection time of a polymer in slit confinement through a nano-pore in the Odijk regime, theoretically and by using computer simulations. This problem is not investigated previously, to the authors' knowledge. In our simulations results, all the error-bars were relatively large, indicating a requirement for longer simulations for measuring the force and the radius of gyration. Also, more simulations are needed to reduce the error-bars of the ejection times.

REFERENCES

[1] Liu, X.; Skanata, M. M.; Stein, D., Entropic cages for trapping DNA near a nanopore. *Nature Communications,* **2015**, *6*, 6222. DOI: 10.1038/ncomms7222.

[2] Cadinu, P.; Paulose Nadappuram, B.; Lee, D. J.; Sze, J. Y.; Campolo, G.; Zhang, Y.; Shevchuk, A.; Ladame, S.; Albrecht, T.; Korchev, Y.; Ivanov, A. P., Single molecule trapping and sensing using dual nanopores separated by a zeptoliter nanobridge. *Nano Lett.,* **2017**, *17*, pp.6376-6384. DOI: 10.1021/acs.nanolett.7b03196.

[3] Di Ventra, M.; Taniguchi, M., Decoding DNA, RNA and peptides with quantum tunnelling. *Nat. Nanotechnol.,* **2016**, *11*, 117. DOI: 10.1038/nnano.2015.320.

[4] Restrepo-Pérez, L.; Joo, C.; Dekker, C., Paving the way to single-molecule protein sequencing. *Nat. Nanotechnol.,* **2018**, *13*, 786-796. DOI: 10.1038/s41565-018-0236-6.

[5] Nikoofard, N.; Fazli, H., A flexible polymer confined inside a cone-shaped nano-channel. *Soft Matter,* **2015**, *11*, 4879-4887. DOI: 10.1039/C5SM00818B.

[6] Rubinstein, M.; Colby, R. H., Polymer Physics (Vol. 23). New York: Oxford University Press, 2003.

[7] Nikoofard, N.; Hoseinpoor, S. M.; Zahedifar, M., Accuracy of the blob model for single flexible polymers inside nanoslits that are a few monomer sizes wide. *Phys. Rev. E,* **2014**, *90*, 062603. DOI: 10.1103/PhysRevE.90.062603.

[8] Hoseinpoor, S. M.; Nikoofard, N.; Zahedifar, M., Accuracy limits of the blob model for a flexible polymer confined inside a cylindrical nano-channel. *J. Statistical Phys.,* **2016**, *163*, 593-603. DOI: 10.1007/s10955-016-1489-9.

[9] Sakaue, T.; Raphaël, E., Polymer chains in confined spaces and flow-injection problems: some remarks. *Macromolecules,* **2006**, *39*, 2621-2628. DOI: 10.1021/ma0514424.

[10] Poier, P.; Likos, C. N.; Matthews, R., Influence of rigidity and knot complexity on the knotting of confined polymers. *Macromolecules,* **2014**, *47*, 3394-3400. DOI: 10.1021/ma5006414.

[11] Möbius, W.; Frey, E.; Gerland, U., Spontaneous unknotting of a polymer confined in a nanochannel. *Nano Lett.,* **2008**, *8*, 4518-4522. DOI: 10.1021/nl802559q.

[12] Reisner, W.; Morton, K. J.; Riehn, R.; Wang, Y. M.; Yu, Z.; Rosen, M.; Austin, R. H., Statics and

dynamics of single DNA molecules confined in nanochannels. *Phys. Rev. Lett*., **2005**, *94*, 196101. DOI: 10.1103/PhysRevLett.94.196101.

[13] Tang, J.; Levy, S. L.; Trahan, D. W.; Jones, J. J.; Craighead, H. G.; Doyle, P. S., Revisiting the conformation and dynamics of DNA in slitlike confinement. *Macromolecules*, **2010**, *43*, 7368-7377. DOI: 10.1021/ma101157x.

[14] Polson, J. M., Free energy of a folded semiflexible polymer confined to a nanochannel of various geometries. *Macromolecules*, **2018**, *51*, 5962-5971. DOI: 10.1021/acs.macromol.8b01148.

[15] Tree, D. R.; Reinhart, W. F.; Dorfman, K. D., The Odijk regime in slits. *Macromolecules,* **2014**, *47*, 3672-3684.

[16] Sakaue, T., Semiflexible polymer confined in closed spaces. *Macromolecules*, **2007**, *40*, 5206-5211. DOI: 10.1021/ma070594r.

[17] Nikoubashman, A.; Vega, D. A.; Binder, K.; Milchev, A., Semiflexible polymers in spherical confinement: Bipolar orientational order versus tennis ball states. *Phys. Rev. Lett*., **2017**, *118*, 217803. DOI: 10.1103/PhysRevLett.118.217803

[18] Milchev, A.; Egorov, S. A.; Binder, K., Semiflexible polymers confined in a slit pore with attractive walls: two-dimensional liquid crystalline order versus capillary nematization. *Soft Matter*, **2017**, *13*, 1888-1903. DOI: 10.1039/C7SM00105C

[19] Dai, L.; Renner, C. B.; Doyle, P. S., Metastable knots in confined semiflexible chains. *Macromolecules*, **2015**, *48*, 2812-2818. DOI: 10.1021/acs.macromol.5b00280

[20] Shin, J.; Cherstvy, A. G.; Metzler, R., Polymer looping is controlled by macromolecular crowding, spatial confinement, and chain stiffness. *ACS Macro Lett.*, **2015**, *4*, 202-206. DOI: 10.1021/ mz500709w

[21] Leith, J. S.; Kamanzi, A.; Sean, D.; Berard, D.; Guthrie, A. C.; McFaul, C. M.; Leslie, S. R., Free energy of a polymer in slit-like confinement from the odijk regime to the bulk. *Macromolecules*, **2016**, *49*, 9266-9271. DOI: 10.1021/ acs.macromol.6b01805.

[22] Taloni, A.; Yeh, J. W.; Chou, C. F., Scaling theory of stretched polymers in nanoslits. *Macromolecules,* **2013**, *46*, 7989-8002. DOI: 10.1021/ma4010549.

[23] Lee, Y. L.; Hsiao, P. Y., Scaling behavior of neutral and charged polymers in nanochannel confinement. *J. Phys. Soc. Japan*, **2018**, *87*, 073801; Dai, L.; Jones, J. J.; van der Maarel, J. R.; Doyle, P. S., A systematic study of DNA conformation in slitlike confinement. *Soft Matter,* **2012**, *8*, 2972-2982. DOI: 10.1021/ma500326w.

[24] Molineux, I. J.; Panja, D., Popping the cork: mechanisms of phage genome ejection. *Nat. Rev. Microbiol.,* **2013**, *11*, 194. DOI: 10.1038/ nrmicro2988.

[25] Muthukumar, M., Polymer translocation. CRC press, 2016.

[26] Heerema, S. J.; Dekker, C., Graphene nanodevices for DNA sequencing. *Nat. Nanotechnol.,* **2016**, *11*, 127. DOI: 10.1038/NNANO.2015.307.

[27] Si, W.; Zhang, Y.; Sha, J.; Chen, Y., Controllable and reversible DNA translocation through a single-layer molybdenum disulfide nanopore. *Nanoscale*, **2018**, *10*, 19450-19458. DOI: 10.1039/ C8NR05830J.

[28] Katkar, H. H.; Muthukumar, M., Role of non-equilibrium conformations on driven polymer translocation. *J. Chem. Phys.,* **2018**, *148*, 024903. DOI: 10.1063/1.4994204.

[29] Sarabadani, J.; Ala-Nissila, T., Theory of pore-driven and end-pulled polymer translocation dynamics through a nanopore: An overview. *Journal of Physics: Condensed Matter*, **2018**, *30*, 274002. DOI: 10.1088/1361-648X/aac796

[30] Nikoofard, N.; Mashaghi, A., Topology sorting and characterization of folded polymers using nano-pores. *Nanoscale*, **2016**, *8*, 4643-4649. DOI: 10.1039/C5NR08828C

[31] Johnson, R. P.; Fleming, A. M.; Perera, R. T.; Burrows, C. J.; White, H. S., Dynamics of a DNA mismatch site held in confinement discriminate epigenetic modifications of cytosine. *J. Am. Chem. Soc.*, **2017**, *139*, 2750-2756. DOI: 10.1021/ jacs.6b12284

[32] Hepp, C.; Maier, B., Kinetics of DNA uptake during transformation provide evidence for a translocation ratchet mechanism. *Proceedings of the National*

Academy of Sciences, **2016**, *113*, 12467-12472. DOI: 10.1073/pnas.1608110113.

[33] He, Y.; Tsutsui, M.; Scheicher, R. H.; Miao, X. S.; Taniguchi, M., Salt-gradient approach for regulating capture-to-translocation dynamics of dna with nanochannel sensors. *ACS Sensors*, **2016**, *1*, 807-816. DOI: 10.1021/acssensors.6b00176.

[34] Jeon, B. J.; Muthukumar, M., Electrostatic control of polymer translocation speed through α-hemolysin protein pore. *Macromolecules*, **2016**, *49*, 9132-9138. DOI: 10.1021/acs.macromol.6b01663.

[35] Panja, D.; Barkema, G. T., Simulations of two-dimensional unbiased polymer translocation using the bond fluctuation model. *J. Chem. Phys.*, **2010**, *132*, 014902. DOI: 10.1063/1.3281641.

[36] Sarabadani, J.; Ikonen, T.; Mökkönen, H.; Ala-Nissila, T.; Carson, S.; Wanunu, M., Driven translocation of a semi-flexible polymer through a nanopore. *Scientific Reports*, **2017**, *7*, 7423. DOI: 10.1038/s41598-017-07227-3.

[37] Palyulin, V. V.; Ala-Nissila, T.; Metzler, R., Polymer translocation: the first two decades and the recent diversification. *Soft Matter*, **2014**, *10*, 9016-9037. DOI: 10.1039/C4SM01819B.

[38] Cacciuto, A.; Luijten, E., Confinement-driven translocation of a flexible polymer. *Phys. Rev. Lett.*, **2006**, *96*, 238104. DOI: 10.1103/PhysRevLett.96.238104.

[39] Huang, H. C.; Hsiao, P. Y., Scaling behaviors of a polymer ejected from a cavity through a small pore. *Phys. Rev. Lett.*, **2019**, *123*, 267801. DOI: 10.1103/PhysRevLett.123.267801.

[40] Matthews, R.; Louis, A. A.; Yeomans, J. M., Knot-controlled ejection of a polymer from a virus capsid. *Phys. Rev. Lett.*, **2009**, *102*, 088101. DOI: 10.1103/PhysRevLett.102.088101.

[41] Abdolvahab, R. H.; Ejtehadi, M. R.; Metzler, R., Sequence dependence of the binding energy in chaperone-driven polymer translocation through a nanopore. *Phys. Rev. E*, **2011**, *83*, 011902. DOI: 10.1103/PhysRevE.83.011902.

[42] Marenduzzo, D.; Micheletti, C.; Orlandini, E., Topological friction strongly affects viral DNA ejection. *Proceedings of the National Academy of Sciences,* **2013**, *110*, 20081-20086. DOI: 10.1073/pnas.1306601110.

[43] Polson, J. M.; Heckbert, D. R., Polymer translocation into cavities: Effects of confinement geometry, crowding, and bending rigidity on the free energy. *Phys. Rev. E,* **2019**, *100*, 012504. DOI: 10.1103/PhysRevE.100.012504.

[44] Sun, L. Z.; Luo, M. B.; Cao, W. P.; Li, H., Theoretical study on the polymer translocation into an attractive sphere. *J. Chem. Phys.*, **2018**, *149*, 024901. DOI: 10.1063/1.5025609.

[45] Berndsen, Z. T.; Keller, N.; Grimes, S.; Jardine, P. J.; Smith, D. E., Nonequilibrium dynamics and ultraslow relaxation of confined DNA during viral packaging. *Proceedings of the National Academy of Sciences*, **2014**, *111*, 8345-8350. DOI: 10.1073/pnas.1405109111.

[46] Odijk, T., The statistics and dynamics of confined or entangled stiff polymers. *Macromolecules*, **1983**, *16*, 1340-1344. DOI: 10.1021/ma00242a015.

[47] Limbach, H. J.; Arnold, A.; Mann, B. A.; Holm, Ch., ESPResSo-An extensible simulation package for research on soft matter systems, *Computational Phys. Commun*. **2006**, *174*, 704-727, DOI: 10.1016/j.cpc.2005.10.005.